A Modified Sensorless Control of Induction Motor Based on Reactive Power

Vladan R. Jevremović, Veran Vasić, Darko P. Marčetić, and Borislav Jeftenić

***Abstract*—This paper presents a modified model reference adaptive system (MRAS) speed estimator for induction motors (IM), based on the instantaneous rotor magnetizing reactive power. The proposed estimator does not use integration in the reference model and it is insensitive to the stator resistance variations. The introduced changes allow analytical tuning of the adaptation mechanism and facilitate implementation of the estimator in a digital signal processor (DSP). The robustness and accuracy of the proposed scheme were verified experimentally for a wide speed range and variable level of rotor flux.**

***Index Terms*—Induction motor drives, model reference adaptive systems, observers, control.**

I. Introduction

MRAS observers consist of a reference model, an adjustable model and an adaptation mechanism, which adapts the speed estimate based on the error between the two model outputs. The classical rotor flux-based MRAS speed estimation [1] is popular because of its simplicity. The main disadvantages of this estimator are poor low-speed operation due to the existence of pure integrators (which introduces problems of initial conditions, offset, drift and integrator saturation), and sensitivity to the variations in stator resistance. The problem of pure integration can be overcome either by replacing integrators with low-pass filters (quasi-integrators) or by using advanced integration methods. Other solutions have employed rotor back electromotive force (EMF)-based MRAS estimators [2, 3], which improve low-speed performance, but suffer from noise in the back-EMF estimate at high speeds and sensitivity to the stator resistance variations. In [4] a parallel stator resistance and rotor speed identification algorithm has been proposed. Additional answers to the problems of integration and sensitivity to the stator resistance have employed MRAS observers based on the rotor magnetizing reactive power [5, 6]. However, the majority of rotor flux, back-EMF and reactive power-based MRAS techniques suffer from inherent instability in the low-speed regenerative mode, unreliable operation at zero frequency with full-rated toque and sensitivity to the rotor time constant variations. The scheme in [7] employs rotor flux and stator current estimators with a modified slip relation and an additional stator voltage-dependent term as a remedy to low-speed instability. The usage of dot products of rotor flux and stator current [8] or rotor flux and back-EMF [9] as additional adaptation terms in the MRAS error signals and parallel stator resistance estimation has resulted in stable low-speed operation. Initially, MRAS observers had a proportional-integral (PI) regulator as the adaptation mechanism, and first tuning methods were empirical with the regulator gains constrained only by the noise in the system. The first reported analytical tuning [10] suited only certain operating modes and lacked universality. Improved MRAS dynamics and clearly defined analytical tuning of the observer, augmented with a full machine mechanical model, are given in [11] with proportional-integral-differential regulator as an adaptation mechanism. Several references combined good properties of MRAS observer for speed estimation and Luenberger observer for flux-current estimation [12, 13], or MRAS and sliding mode observers [14] that yielded improved dynamics of the estimate. Some authors propose the usage of fuzzy-logic controllers in place of the adaptation mechanism [15], or multi-layer artificial-neural-networks combined with the MRAS reference model [16], where the adaptation mechanism is inside the adjustable model. Although very complex, these solutions reported robust and accurate results. This paper contributes to the improvement of the reactive power-based MRAS speed observer, by identifying an analytical method to define parameters of the adaptation mechanism, resulting in a stable first-order system.

V. R. Jevremović is with Parker SSD Drives, Littlehampton, United Kingdom (e-mail: vladan@rocketmail.com).

V. Vasić and D. P. Marčetić are with the University of Novi Sad, Faculty of Technical Sciences, Novi Sad, Serbia.

B. Jeftenić is the University of Belgrade, Faculty of Electrical Engineering, Belgrade, Serbia.

II. Mathematical Model

An IM in a stationary reference frame can be modeled using complex stator and rotor voltage and flux linkage equations:

$$\begin{aligned} \underline{v}_s &= R_s \underline{i}_s + \dot{\underline{\psi}}_s \\ 0 &= R_r \underline{i}_r + \dot{\underline{\psi}}_r - j\omega_r \underline{\psi}_r \end{aligned} \tag{1}$$

$$\begin{aligned} \underline{\psi}_s &= L_s \underline{i}_s + L_m \underline{i}_r \\ \underline{\psi}_r &= L_m \underline{i}_s + L_r \underline{i}_r \end{aligned} \tag{2}$$

The voltage, current and flux space vectors from previous equations are given as

$$\underline{x} = x_\alpha + jx_\beta \ , \ x \in \{v_s, i_s, i_r, \psi_s, \psi_r\} \tag{3}$$

The IM mechanical subsystem is modeled with

$$J_m \dot{\omega}_{mr} = T_e - T_l - B\omega_{mr} \tag{4}$$

where ω_{mr} is the rotor mechanical angular frequency.

The rotor magnetizing back-EMF $\underline{e}_m$ and current $\underline{i}_m$ vectors are defined as:

$$\underline{e}_m = L_m \underline{\dot{\psi}}_r / L_r \tag{5}$$

$$\underline{i}_m = \underline{\psi}_r / L_m \tag{6}$$

The rotor back-EMF for the reference model is derived from (1), (2) and (5) as

$$\underline{e}_m^v = \underline{v}_s - R_s \underline{i}_s - \sigma L_s \underline{\dot{i}}_s \tag{7}$$

Similarly, the back-EMF for the adjustable model is obtained from (1), (2) and (6) as

$$\underline{e}_m^i = L_m' \underline{\dot{i}}_m = L_m' \left[\frac{1}{\tau_r} \underline{i}_s - \left(\frac{1}{\tau_r} - j\hat{\omega}_r \right) \underline{i}_m \right] \tag{8}$$

where $L_m' = L_m^2 / L_r$ is the equivalent magnetizing inductance and $\tau_r = L_r / R_r$. In the reference and adjustable models, the outputs are rotor magnetizing reactive powers (q_m^v, q_m^i) defined in (9) as the cross product of rotor back-EMF and stator current vector, which removes the integration and dependence on the stator resistance.

$$q_m^k = \vec{i}_s \otimes \vec{e}_m^k = \mathrm{Im}\left\{ \underline{i}_s^* \cdot \underline{e}_m^k \right\}, \quad k = v, i \tag{9}$$

The error $\varepsilon = q_m^v - q_m^i$ between the two models becomes the input to the adaptation mechanism, which gives the estimated $\hat{\omega}_r$ at its output. Fig. 1a depicts the structure of the proposed MRAS speed observer. The reference model output is averaged using a finite impulse response filter (FIR) which suppresses noise from the differentiation of stator currents in (7) and filters out the higher harmonic content. The adjustable model is divided into two sub-models that are described in the further text.

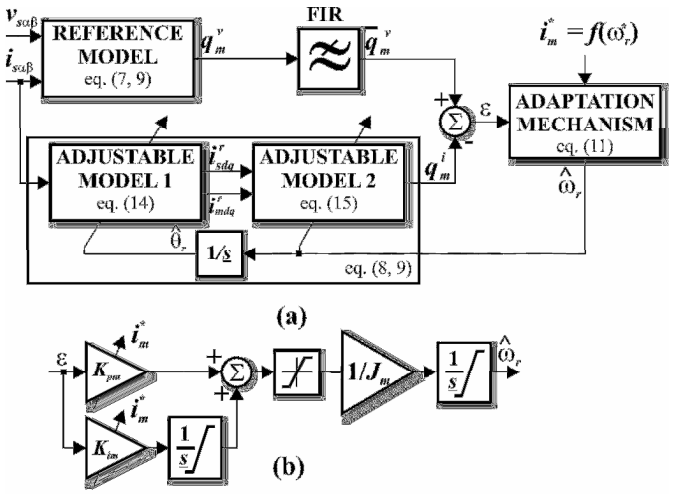

Fig. 1. (a) MRAS speed observer, (b) adaptation mechanism.

III. Adaptation Mechanism

In order to select an appropriate adaptation mechanism, a small-signal model of the MRAS observer has to be devised. Small-signal dynamics of the observer can be modeled by transforming (7)-(9) into a synchronous (d-q) reference frame and by linearizing them around the chosen steady-state point. The general assumptions are that: the synchronous angular frequency ω_e is constant, hence stationary angular slip frequencies are equal ($\omega_{sl0} = \hat{\omega}_{sl0}$); the rotor time constant τ_r is known exactly; the MRAS speed feedback results in equality of steady-state rotor magnetizing currents and zero q-axis component of rotor flux. In addition, all second-order small signals can be neglected. Following these assumptions, the transfer function of the open-loop MRAS observer describes dependence between the small-signal error and rotor speed error (I_{sq0} is a steady-state value of i_{sq}):

$$H_m(\underline{s}) = \frac{\Delta\varepsilon}{\Delta\omega_r - \Delta\hat{\omega}_r} = L_m' I_{mn}^2 \frac{\underline{s}^2 + \left(\frac{1}{\tau_r} + \tau_r \omega_{r0} \omega_{sl0} \right) \underline{s} + 2\omega_e \omega_{sl0}}{\underline{s}^2 + \frac{2}{\tau_r} \underline{s} + \frac{1}{\tau_r^2} + \omega_{sl0}^2} \tag{10}$$

Fig. 1b shows the proposed adaptation mechanism, which comprises a PI regulator (with proportional K_{pm} and integral K_{im} gains) and a simplified mechanical model with motor inertia J_m derived from (4) assuming that the friction and the load torque are neglected ($B \approx 0$, $T_l \approx 0$). The output of the PI regulator is considered proportional to T_e, thus the transfer function of the adaptation system is

$$H_a(\underline{s}) = \frac{K_{pm} \underline{s} + K_{im}}{J_m \underline{s}} \frac{p}{J_m \underline{s}} \tag{11}$$

Assuming $\omega_{sl0} = 0$, one can select parameters of the regulator by using (12), and applying cancellation of the dominant pole in the open-loop transfer function (10). Unlike solutions with PI regulators only, a mechanical model with J_m enables cancellation of a single zero in the open-loop transfer function that may exacerbate the noise at high frequencies and render the system unstable. The resulting transfer function of closed-loop speed observer (13) gives a stable system in the form of a first-order low-pass filter with a cut-off frequency $\omega_c = 2\pi f_c$.

$$K_{pm} = \frac{\omega_c J_m}{p L_m' I_{mn}^2} \approx \frac{\omega_c J_m}{p L_m' i_m^{*2}}, \quad K_{im} = K_{pm} / \tau_r \tag{12}$$

$$H(\underline{s}) = \frac{\Delta\hat{\omega}_r}{\Delta\omega_r} = \frac{H_m(\underline{s}) H_a(\underline{s})}{1 + H_m(\underline{s}) H_a(\underline{s})} = \frac{\omega_c}{\underline{s} + \omega_c} \tag{13}$$

The frequency f_c is selected to be 2–10 Hz. In order to generalize the regulator gains K_{pm} and K_{im} over a wide speed range and to maintain the desired bandwidth, the regulator employs gain scheduling such that I_{mn} in (12) is replaced with the reference magnetizing current as a function of the

reference rotor speed, i.e. $i_m^* = f(\omega_r^*)$. The τ_r in (12) is set to its rated value τ_{rn}.

IV. Experimental Results

The proposed speed-observer was verified by using an experimental setup consisting of 2 kW DC machine (posing as an active load), IM and 1.2 kW inverter, which are controlled using an indirect field oriented control topology, as shown in Fig. 2. The IM parameters were – rated power P_n = 750 W, rated voltage V_n = 195 V_{rms}, rated frequency f_n = 70 Hz, star connected stator, p = 1, R_s = 3.03 Ω, R_r = 1.89 Ω, L_s = L_r = 184 mH, L_m = 172 mH, σL_s = 21.91 mH, and $J_m = 3.53\times10^{-4}$ kgm^2.

The IM was driven by a 3-phase current-controlled voltage source inverter, which operated at 10 kHz switching frequency (the frequency was randomized ± 10% around this value) and used space vector pulse-width modulation (SVPWM) with a rated DC link voltage of 340 V. All control and estimation algorithms were implemented in a Texas Instrument DSP TMS320F2810 operating at 125 MHz. The current regulators were implemented in a synchronous reference frame and updated at the PWM rate. The bandwidth of the current loop was set to 250 Hz and incorporated decoupling terms updated at 1 kHz. The motor voltages were estimated using the DC link voltage samples and the PWM duty cycles with dead-time and IGBT voltage drops compensation. The flux and slip frequency estimators along with the flux regulator were running at 1 kHz, with the flux loop bandwidth set to 90 Hz. The speed loop was running at a 1ms sample rate with the bandwidth of 10 Hz. The IM speed was monitored via an incremental encoder. The reference model of the MRAS observer was updated at the PWM rate. The adjustable model 1 was running at the PWM rate and estimated the rotor magnetizing current in a rotor reference frame according to (14), which made the model independent of $\hat{\omega}_r$ and provided the additional filtering through integration.

$$\underline{i}_m^r = \frac{1}{\hat{\tau}_r}(\underline{i}_s^r - \underline{i}_m^r) \tag{14}$$

The rotor magnetizing $\underline{i}_m^r$ and stator currents vectors $\underline{i}_s^r$ were obtained from $\underline{i}_m$ and $\underline{i}_s$ in a stationary reference frame, through rotational transformations using $\hat{\theta}_r$. The adjustable model 2, was running at a 1ms rate and gave the rotor reactive power as

$$q_m^i = L_m'\left[\hat{\omega}_r\left(i_{md}^r i_{sd}^r + i_{mq}^r i_{sq}^r\right) + \frac{1}{\tau_r}\left(i_{md}^r i_{sq}^r - i_{mq}^r i_{sd}^r\right)\right] \tag{15}$$

The adaptation mechanism was running every 1ms with its output integrated every PWM interval in order to obtain the estimated rotor position $\hat{\theta}_r$. Since the MRAS estimator behaved as a low-pass filter, it was necessary to compensate for the introduced phase lag. If the slip frequency is neglected, the estimated rotor position is

$$\hat{\theta}_r = \int \hat{\omega}_r dt + \tan^{-1}(\hat{\omega}_r / \omega_c) \tag{16}$$

The IM magnetizing curve was experimentally determined and feed-forward compensation of saturation effects [17] was applied. The transient stator inductance σL_s is considered constant and any error in this value may become dominant at high frequencies. The proposed speed observer was tested for the entire speed region. Fig. 3 illustrates the waveforms of the rotor reactive powers, d and q-axis stator currents; measured and estimated rotor speeds with the IM running in the base speed region, for a reference speed of 540 rpm at the rated load of 1 Nm. The power q_m^v has a significant amount of high-frequency noise that originates from the differentiation of stator currents. The stator d-axis current i_{sd} is kept at the rated value, which corresponds to the rated i_m current, whilst $\hat{\omega}_r$ tracks the actual rotor speed with minimal latency and zero steady-state error. Fig. 4 depicts the waveforms of reactive powers, i_{sd} and i_{sq} currents and rotor speeds for the IM operating in the field-weakening region, once it reached the reference speed of 6300 rpm at 0.5 Nm load torque. The reference reactive power drops faster than the i_{sd} current and the harmonic content in the reactive power estimates becomes significantly higher. The estimate $\hat{\omega}_r$ accurately matches the real speed, with a marginal steady-state error. Fig. 5 shows the relevant waveforms for low-speed operation at 60 rpm and 1 Nm load. The average $\hat{\omega}_r$ matches the actual speed after 400 ms, with a significant ripple in the instantaneous value. The minimal achieved rotor frequency using the proposed estimator is 0.25 Hz at rated load, whilst the maximum speed is 210 Hz.

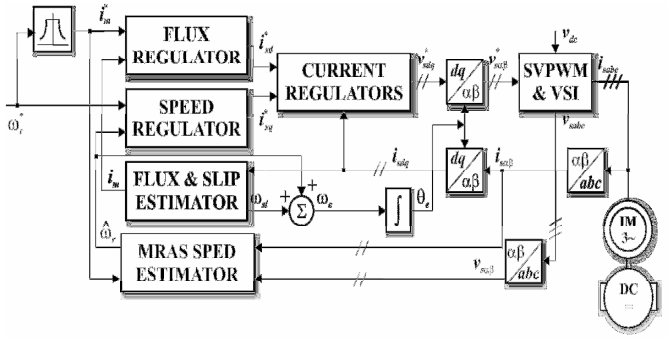

Fig. 2. Experimental setup.

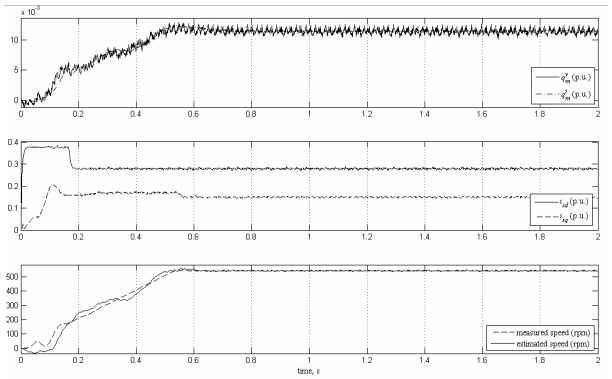

Fig. 3. Waveforms for the base speed region.

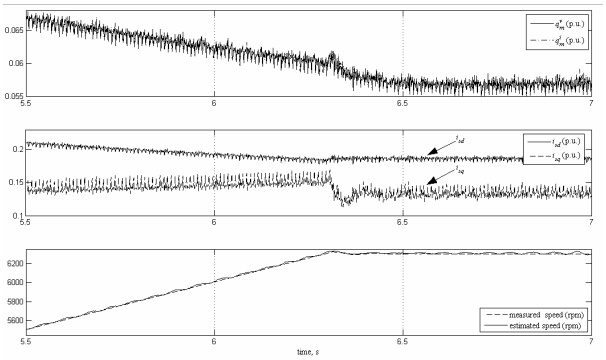

Fig. 4. Waveforms for the field-weakening region.

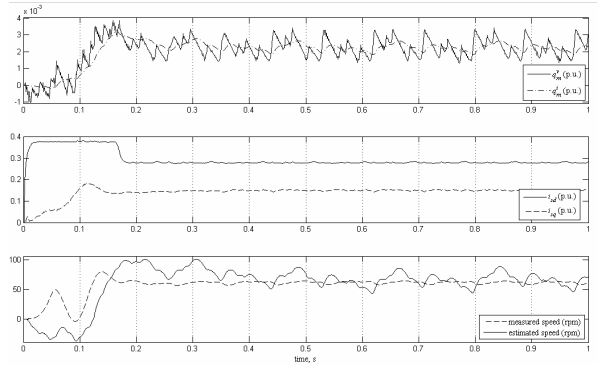

Fig. 5. Waveforms for 1 Hz reference frequency.

V. Conclusion

This paper describes a modified speed-sensorless control of an IM based on rotor reactive power. The proposed technique does not require integrators in the reference model; it is robust to the stator resistance variations, and operates reliably over a wide speed range. The observer is augmented with a simple mechanical model of the IM that helps to construct a more effective speed adaptation mechanism and enables its analytical tuning. The proposed scheme was verified experimentally and the overall system exhibited robustness and satisfactory accuracy over a wide speed range.

Appendix

v_s, e_m – stator voltage and rotor back-EMF
i_s, i_r, i_m – stator, rotor and rotor magnetizing current
ψ_s, ψ_r – stator and rotor flux
R_s, R_r – stator and rotor resistance
L_s, L_r, L_m – stator, rotor and magnetizing inductance
τ_r – rotor time constant
σ – total leakage coefficient, $\sigma = 1 - L_m^2/(L_s L_r)$
ω_r, $\hat{\omega}_r$ – actual and estimated rotor electrical angular frequency
ω_{sl}, $\hat{\omega}_{sl}$ – actual and estimated slip angular frequency
$\hat{\theta}_r$ – estimated rotor electrical position
T_e, T_l – electromagnetic and load torque
J_m, B – motor inertia and friction coefficient
p – number of pole pairs
v, i – reference and adjustable model values (super script)
0 – stationary values (subscript)
Δ – small-signal variations
α, β – stationary reference frame (subscript)
d, q – synchronous reference frame (subscript)
r – rotor reference frame (superscript)
$\dot{x}$ – first derivative (dx/dt)
$\underline{s}$ – complex angular frequency ($j\omega$)

References

[1] C. Schauder, "Adaptive Speed Identification for Vector Control of Induction Motors without Rotational Transducers," IEEE Trans. Ind. Appl., vol. 28, no. 5, pp. 1054–1061, Sep./Oct. 1992.

[2] F. Z. Peng, D. J. Adams, "Speed-Sensorless Control of Induction Motors for Electric Vehicles," in Conf. Rec. SAE Future Car Congress, Batt. and Energy Tech. Sess. (Part D), pp. 1–6, 2000.

[3] M. N. Marwali, A. Keyhani, "A comparative study of rotor flux based MRAS and back EMF based MRAS speed estimators for speed sensorless control of induction machines," in Conf. Rec. 32nd IAS Ann. Meeting, vol. 1, pp. 160–166, 1997.

[4] V. Vasic, S. Vukosavic, E. Levi, "A stator resistance estimation scheme for speed sensorless rotor flux oriented induction motor drives," IEEE Trans. Energy Conv., vol. 18, no. 4, pp. 476–483, Dec. 2003.

[5] F. Z. Peng, T. Fukao, "Robust Speed Identification for Speed-Sensorless Vector Control of Induction Motors," IEEE Trans. Ind. Appl., vol. 30, no. 5, pp. 1234–1240, Sept./Oct. 1994.

[6] C. M. Ta, T. Uchida, Y. Hori, "MRAS-based Speed Sensorless Control of Induction Motor Drives Using Instantaneous Reactive Power," in Conf. Rec. of 27th Ann. Conf. IEEE Ind. Electron. Soc. IECON, pp. 1417–1422, 2001.

[7] L. Harnefors, "Instability Phenomena and Remedies in Sensorless Indirect Field Oriented Control," IEEE Trans. Power Electron. , vol. 15, no. 4, pp. 733–743, Jul. 2000.

[8] M. Rashed, F. Stronach, P. Vas, "A Stable MRAS-Based Sensorless Vector Control Induction Motor Drive at Low Speeds," in Conf. Rec. IEEE Electrical Machines and Drives Conference IEMD, vol. 1, pp. 139–144, 2003.

[9] M. Rashed, F. Stronach, "A Stable Back-EMF MRAS-based Low-speed Induction Motor Drive Insensitive to Stator Resistance Variation," in Proc. IET Elec. Power Appl., vol. 151, no. 6, pp. 685–693, 2004.

[10] H. Tajima, Y. Hori, "Speed Sensorless Field-Orientation Control of the Induction Machine," IEEE Trans. Ind. Appl., vol. 29, no. 1, pp. 175–180, Jan./Feb. 1993.

[11] R. Blasco-Gimenez, G. M. Asher, M. Sumner, K. J. Bradley, "Dynamic Performance Limitation for MRAS Based Sensorless Induction Motor Drives – Part 1: Stability Analysis for the Closed Loop Drive," in Proc. IEEE Elect. Power Appl., vol. 143, no. 2, pp. 113–122, Mar. 1996.

[12] G. Griva, F. Profumo, R. Bojoi, V. Bostan, M. Cuius, C. Ilas, "General Adaptation Law for MRAS High Performance for Sensorless Induction Motor Drives," in Conf. Rec. IEEE 32nd Annu. Power Electron. Spec. Conf. PESC, vol. 2, pp. 1197–1202, 2001.

[13] M. Messaoudi, L. Sbita, M. B. Hamed, H. Kraiem, "MRAS and Luenberger Based Sensorless Indirect Vector Control of Induction Motors," Asian J. of Inf. Technol., vol. 7, pp. 232–239, 2008.

[14] M. Comanescu, L. Xu, "Sliding-Mode MRAS Speed Estimators for Sensorless Control of Induction Motor Drive," IEEE Trans. Ind. Electron., vol. 53, no. 1, pp. 146–153, Feb. 2006.

[15] S. M. Gadoue, D. Giaouris, J. W. Finch, "A New Fuzzy Logic Based Adaptation Mechanism for MRAS Sensorless Vector Control Induction Motor Drives," in Proc. 4th IET Power Electron., Mach. and Drives PEMD, 2008, pp. 179–183.

[16] M. Cirrincione, M. Pucci, "An MRAS-Based Sensorless High-Performance Induction Motor Drive with a Predictive Adaptive Model," IEEE Trans. Ind. Electron., vol. 52, no. 2, pp. 532–551, Apr. 2005.

[17] E. Levi, M. Wang, "A Speed Estimator for High Performance Sensorless Control of Induction Motors in the Field Weakening Region," IEEE Trans. Power Electron., vol. 17, no. 3, pp. 365–378, May 2002.